ANALELE UNIVERSITĂŢII
"EFTIMIE MURGU" REŞIŢA
ANUL XXI, NR. 3, 2014, ISSN 1453 - 7397

Constantin Vlad Suru, Mihaita Linca, Cristina Alexandra Patrascu

Evaluation of Current Control Methods in Three-Phase Shunt Active Power Filters System

This paper aims the implementation of the control techniques for shunt power active filters and the achievement of a comparative study regarding the performance achieved by these techniques both in simulation and on an experimental active filter. The experimental active filter is using the dSpace DS1103 DSP board for the control section so different methods for the compensating current computation as well as for the DC-Link voltage and output current control can be investigated.

Keywords: DSP, harmonic distortion, current decomposition, active compensator

1. Introduction

The shunt power active compensators requires for their operation the use of control loops in order to obtain both the instantaneous value of the compensating current and the voltage on the compensation capacitor. Usually, hysteresis regulators are used for the current control and PI controllers for the voltage control, but the latest research trends are to replace the hysteresis current controllers with PI regulators using the triangular carrier PWM modulation. The feasibility of this transition is investigated in this paper.

Further in the paper, the 2nd section presents the adopted compensating current computation method, in this study, the Conservative Power Theory. The 3rd section describes the closed loop current control techniques which are to be investigated. The Simulink model of the virtual active filtering system is presented in the 4th section, in which the simulation results are also described, for a typical nonlinear load, and the power quality indicators. The 5th section presents the experimental setup as well as the experimental results, in order to validate the virtual results and to have a complete image of the study. Finally, the 6th section is for conclusions.

2. Reference current computation using CPT.

In order to calculate the compensating current, the CPT theory was used, where the active and reactive currents are defined in such way so they are equivalent to a balanced load absorbing the same active power and reactive energy of the actual load [1].

Each current component was defined as follows [1]:

- Balanced active current:

$$\underline{i}_a^b = \frac{\boldsymbol{P}}{\boldsymbol{U}^2}\underline{u} = G^b\underline{u}, \tag{1}$$

where:

- G^b is the equivalent balanced conductance.
- Balanced reactive current:

$$\underline{i}_r^b = \frac{\langle \hat{\underline{u}}, \underline{i} \rangle}{\left\| \hat{\underline{u}} \right\|^2}\hat{\underline{u}} = \frac{\boldsymbol{W}}{\hat{\boldsymbol{U}}^2}\hat{\underline{u}} = B^b\hat{\underline{u}} \tag{2}$$

where:

- $\langle \hat{u}, i \rangle = \frac{1}{T}\int_0^T \hat{u} \cdot i \, dt$ is the internal product;
- $\hat{u} = \mu \cdot \left(\int_0^t u(\tau) d\tau - \frac{1}{T}\int_0^T \int_0^t u(\tau) d\tau dt \right)$ is the time integral;
- W is the three-phase reactive energy absorbed by the load and B^b is the equivalent balanced susceptance.

The compensating current will be calculated from the load current depending on the compensation goals, as follows:

- Unity power factor – the active filter will compensate the entire non-active current:

$$\underline{i}_F^* = \underline{i}_L - \underline{i}_a \tag{3}$$

- harmonics compensation – the active filter will compensate only the distorted component:

$$\underline{i}_F^* = \underline{i}_L - \underline{i}_a - \underline{i}_r \tag{4}$$

3. Active filters control methods.

The active filters performances depend on the reference currents computation method as well as on the current and voltage control loops [2][3]. The block diagram of the inner current loop and of the outer voltage loop is illustrated in Fig. 1.

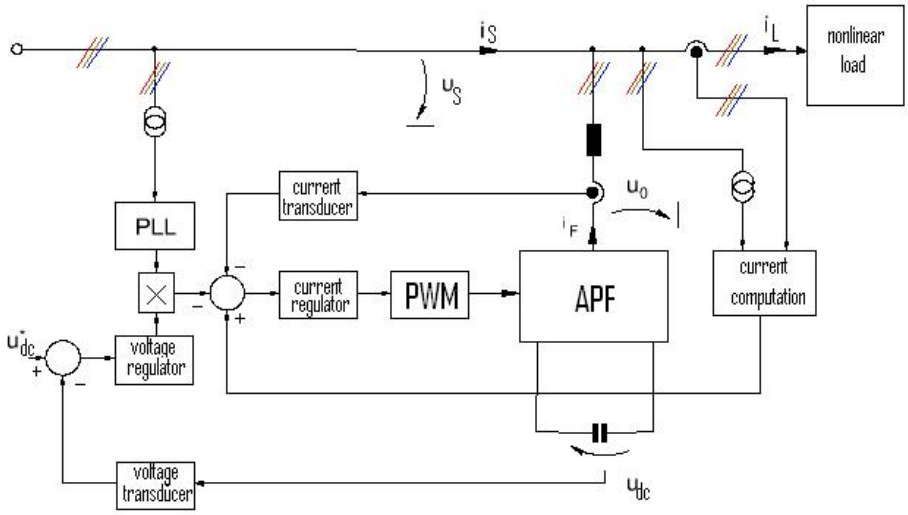

Figure 1. The active filtering system block diagram.

The voltage control loop is necessary to maintain the compensating capacitor voltage to an imposed value, dependant on the power to be compensated. The voltage regulator is always a PI regulator, its output being the amplitude of the active current to be absorbed by the active filter (to charge the compensating capacitor to the working voltage and to cover the power inverter losses). This active current is obtained multiplying the voltage regulator output by a unitary amplitude current in phase with the grid voltage. The voltage loop operation directly influences the performance of the active filter [3].

Regarding the inner current loop, two current controllers are typically adopted:

- hysteresis current controller
- PI current controller.

The first case is widely adopted because of the hysteresis controller simplicity and robustness. In this case, no regulator tuning is required, the controller operation is not affected by the system structure changes, but the working frequency is variable and dependent on the current slope [5].

The second case is rarely used because the PI regulator tuning process is difficult, and the current loop operation with the voltage loop can cause problems. On the other side, the working frequency is constant, which is an advantage in the power inverter and interface filter design. So, the PI current controller, correctly tuned, can give very good results [2].

4. Virtual implementation of the active filtering system

Because the results obtained by simulation are compared to the experimental results, in order to have a relevant comparison, the virtual system has the same components as the experimental one, grouped in masked blocks.

4.1. The Simulink Model of the active filtering system

The virtual model is a Matlab Simulink model containing all the components in Fig. 1, and it was constructed using SymPowerSystems blocks for the power section (like the power inverter, the interface filter, the nonlinear load, etc). The model main components are: the power inverter (with 100A, 1200V IGBTs); the interface filter (first order inductive filter, L=4.4mH); the compensating capacitor (C=1100μF / 800V); the nonlinear load (three-phase full wave rectifier connected to the power grid through a Y-Y transformer 380/240V); the control algorithm of the active filter which is a distinct Simulink block which contains all the necessary computing blocks for the implementation of the [6]:

- Compensating current computation using the CPT;
- The output current and the DC-Link voltage regulating loops;
- Auxiliary blocks for the active filter start-up process control.

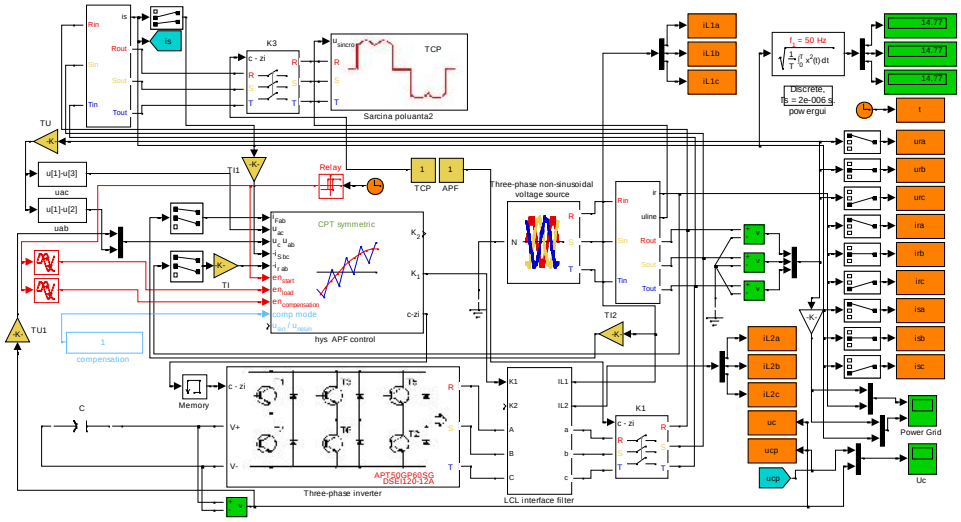

Figure 2. The active filtering system virtual implementation

4.2. The virtual system results

The virtual determinations were obtained considering the following initial conditions:

- The DC-Link voltage control loop is the same for the both current control methods (hysteresis and PWM).
- The power grid voltage is non-sinusoidal – the voltage THD is 4.47%;
- The current absorbed by the nonlinear load was set at 15A on each phase.
- Because of the high slope of the rectifier current, measured at the PCC despite the transformer inductance, after the compensation the current still retain these slopes, for the 4.4mH interface filter. Consequently, the current total harmonic factor is altered and the comparison between the filter current control methods cannot be accomplished. In order to solve this problem, series reactances were added to reduce the rectifier current slope. In this case, the load current THD is 22.34%.

The power grid voltages and currents without compensation, considering these conditions, are illustrated in Fig. 3. From the harmonic spectrum of the load current in Fig. 4 it can be observed that the important harmonics are the 5^{th}, 7^{th}, 11^{th} and 13^{th}, all other harmonics being insignificant.

4.2.1 The hysteresis current controllers

When the hysteresis current controllers were put to the test, the compensated current waveform that has resulted, for the partial compensation, can be observed in Fig. 5. The hysteresis band was calculated using [5]:

$$hys = 2\frac{U_{DC-Link}}{8 \cdot f_{sw\ max}}, \tag{5}$$

where the considered maximum value of the switching frequency is 7500 Hz and the DC-Link operating voltage is 700 V, giving a hysteresis band of 58.3 mA.

In order to have relevant results, the maximum simulation step-time was restricted to the dSpace time step (which is 20μs), so the resulted hysteresis band exceeded the prescribed value to about 4.45 A. The minimum and the maximum switching frequency is 5.42 kHz and 19.2 kHz, respectively. The filtration efficiency is proved by the compensated current waveform and harmonic spectra in Fig. 5, but also by the numerical results synthesized in Table 1.

An interesting fact is that the grid current waveform should take the grid voltage shape, because according to the CPT both waveforms must be similar. This proves not to be true in the first hand from the waveforms (the current is almost sinusoidal despite the voltage, which is flattened). But, on the other hand, it can be seen, that the current harmonics in the first 100 (corresponding to the lowest switching frequency) are practically null.

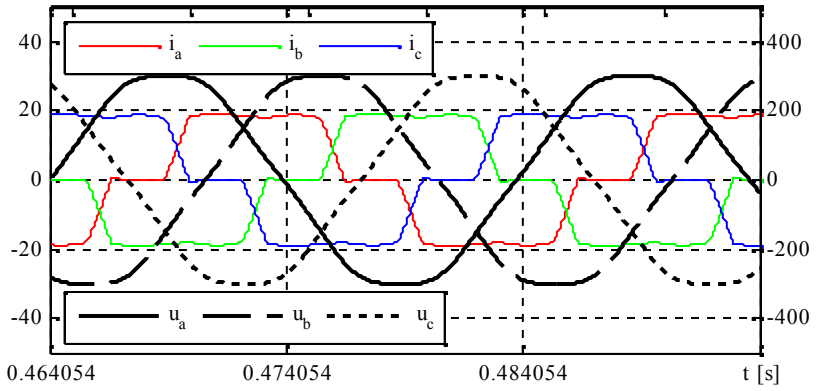

Figure 3. The power grid voltages and currents without compensation

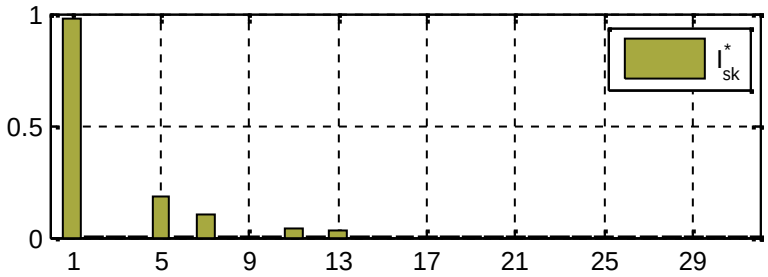

Figure 4. The power nonlinear load current harmonic spectrum

This means that the compensated current is sinusoidal, with a high frequency noise added. This noise is due to the switching operation of the active filter, and is dispersed all over the harmonic spectra. This can be explained by the fact that because of the high time step the hysteresis regulator are not functioning correctly so the switching frequency is no more linearly dependant on the filter current slope.

If the DC-Link voltage control loop is tuned correctly, its influence on the compensated current waveform is negligible. This proves to be so, because the compensated current waveform is not distorted by low frequency harmonics which can be produced by the voltage loop improper functioning. Regarding the current control loop performance, this follows from the difference between the THD and the PHD of the compensated current. This is because the harmonics caused by the switching operation of the active filter are above the 108th harmonic. Therefore, the partial harmonic distortion factor, calculated for the first 51 harmonics shows the performance of the compensated current computation method. The more the THD is higher than the PHD, the more switching harmonics are produced by the active filter and injected into the power grid.

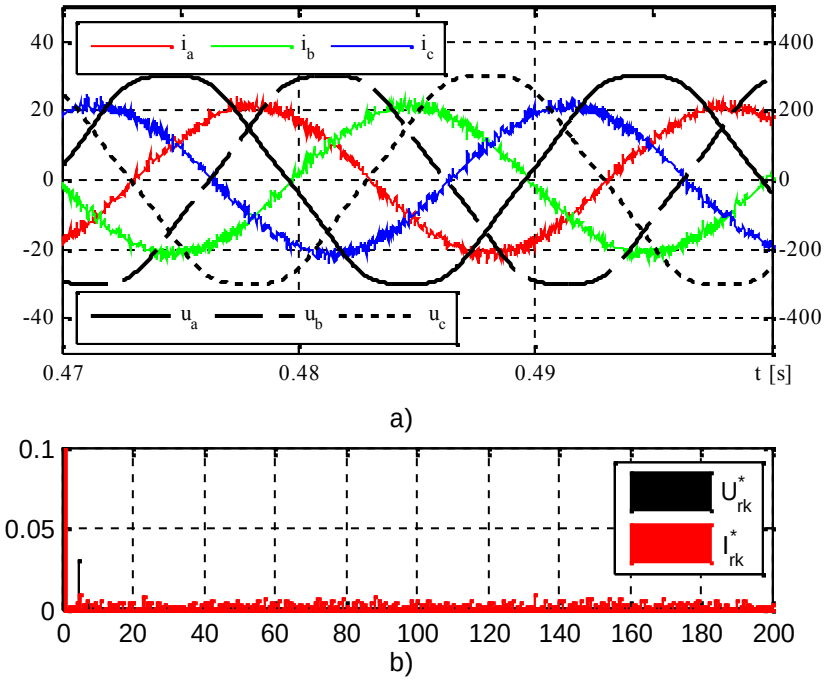

Figure 5 The power grid voltages and currents after partial compensation, for the hysteresis current regulator: a) the waveforms, b) harmonic spectrum

4.2.2. The PI current controllers

When the PI current controllers are used, the gating signals for the power inverter IGBTs are obtained using the triangular carrier modulation. In this case, the current controller output signal is the modulating signal for the PWM modulator. This method has the advantage of the constant switching frequency (which is equal to the carrier signal frequency), but at the same time, the disadvantage of the PI regulator tuning, which is a laborious task.

The compensated current waveform, for the partial compensation, can be observed in Fig. 6-a. In this case, because the switching frequency is constant at 7500 Hz, the current regulating loop is functioning almost correct (the high time step causes the triangular carrier to have small imperfections, but with no high impact on the final result), so the high frequency noise is clearly visible left and right the 150th harmonic (Fig. 6-b), which is the 7500 Hz switching frequency. Again, the imperfections in the carrier shape can be seen in the waveform as well as in the harmonic spectra, mainly in the interval between the 40th to 100th harmonic, but not dispersed on all the spectra, like in the hysteresis case.

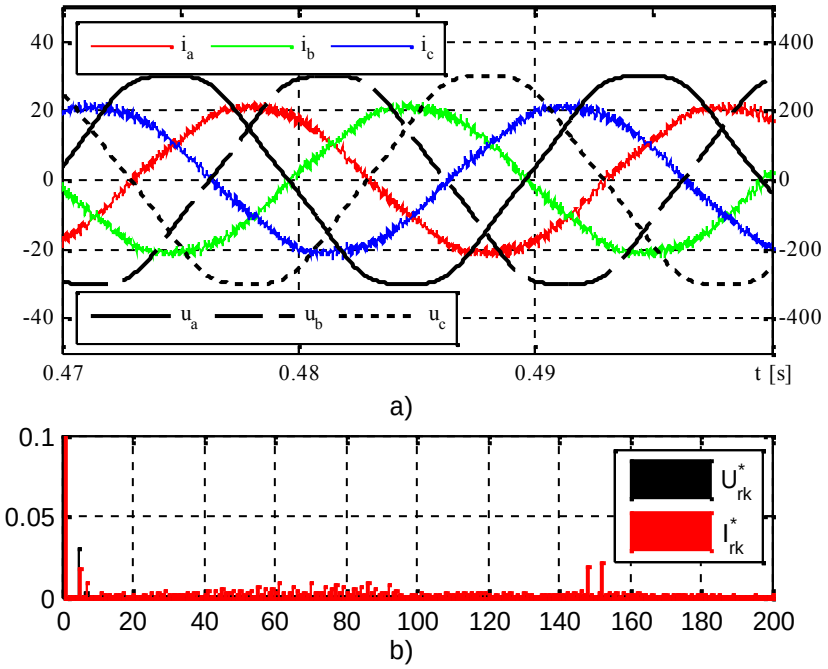

Figure 6. The power grid voltages and currents after the partial compensation, for the PWM current regulator: a) the waveforms, b) harmonic spectrum

This is having a direct effect on the current waveform (the first 51 harmonics), thus the compensated current takes the voltage shape: the current is flattened like the voltage, i.e. the current up to 51th harmonics are reduced close to the voltage corresponding values.

Table 1. Numerical results

Current regulator	THD_{uS} [%]	THD_{iS} [%]	$PHD_{iS\ 51}$	THD_{iL} [%]	FE
Hysteresis	3.11	6.00	2.59	22.35	3.696
PWM		5.61	2.58		3.98

5. The experimental active filtering system

The experimental filtering system was obtained joining two sections: the hardware section which includes all the power components, interface electronics, wiring and the necessary transducers, and also, the software section, which includes the compensating current computation and the voltage and current control loops.

5.1. Experimental setup

The experimental system can be divided in two sections:

- The hardware section which includes: the three-phase power inverter; the first order interface filter; the compensating capacitor in the DC-Link; the polluting load (in fact, a three-phase thyristor rectifier connected to the power grid through a Y-Y adapting transformer).
- The software section which is a masked Simulink block containing all the necessary computing blocks for the compensating current method, and the control algorithm of the active compensator (two control loops).

In order to control the hardware section using the software section an interface between them is necessary. This interface is a virtual control panel which contains all the necessary virtual instruments as a real panel (switches, indicator lamps, panel meters, etc) [7].

5.2. Experimental results

The experimental determinations were performed considering the same initial conditions as in simulation: the DC-Link voltage control loop has the same structure and the same parameter values of the PI controller for both control methods; the power grid voltage is non-sinusoidal, having the THD of 2.09%; the current absorbed by the nonlinear load was set at 15A; the load current THD with the line inductors is 15.77%.
The power grid voltages and currents without compensation, considering these conditions, are illustrated in Fig.7 and the harmonic spectra of the current in Fig.8.

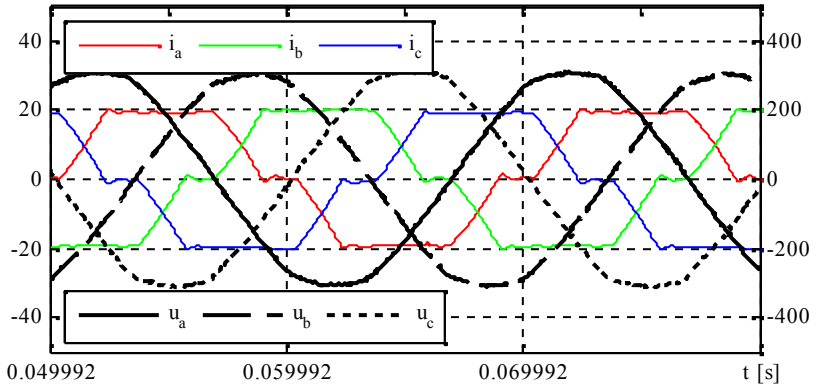

Figure 7. The power grid voltages and currents without compensation

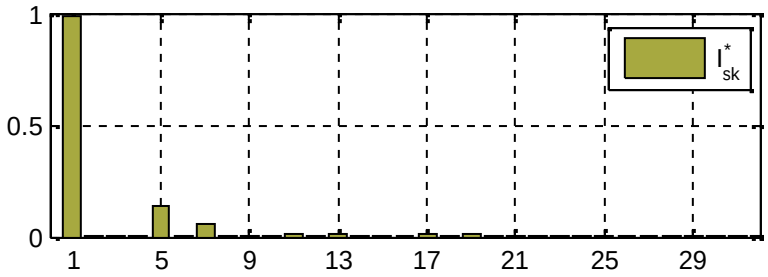

Figure 8. The power grid current harmonic spectrum without compensation

5.2.1 The hysteresis current controllers

The hysteresis band of the current regulators has the same value as in the simulation case, being calculated for the same conditions. Because the lowest sampling rate of the dSpace DS1103 control board is limited to 20 μs, the real hysteresis band exceeded the prescribed value to about 2.14 A. The minimum and the maximum switching frequency is 5.71 kHz and 11.43 kHz, respectively.
The grid voltages and currents after the compensation are illustrated in Fig. 9.

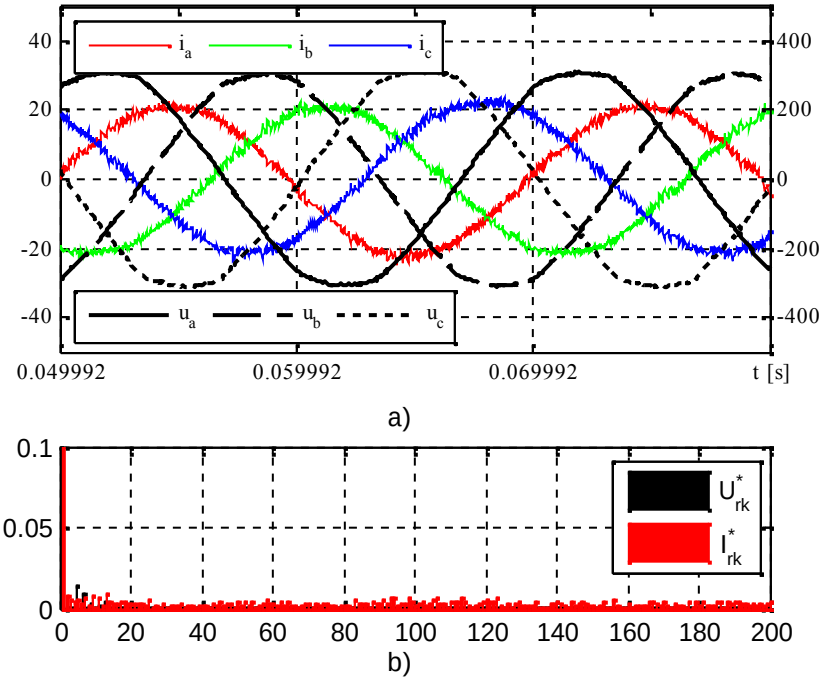

Figure 9. The power grid voltages and currents after the partial compensation, for the hysteresis current regulator: a) the waveforms, b) harmonic spectrum

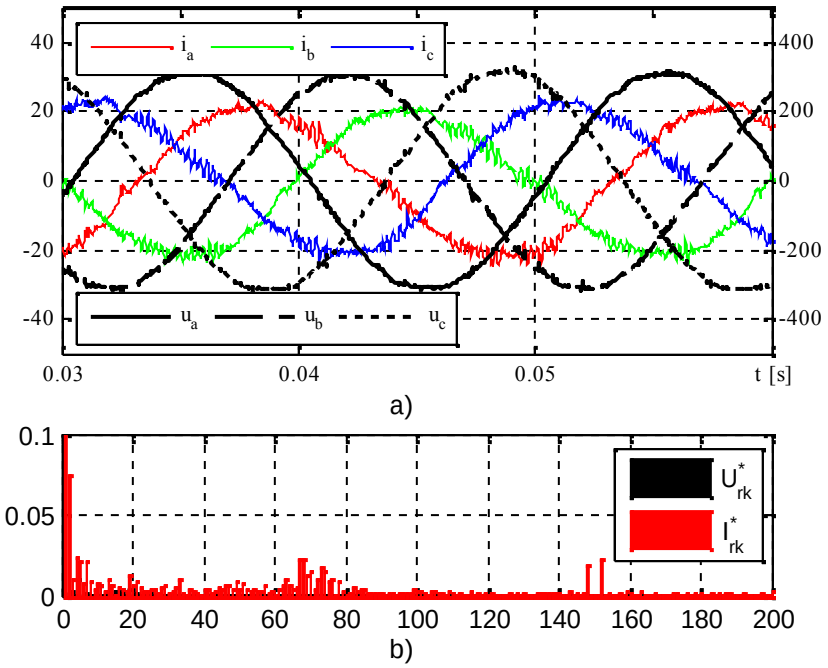

Figure 10. The power grid voltages and currents after the partial compensation, for the PWM current regulator: a) the waveforms, b) harmonic spectrum

The power quality indicators are synthesized in Table 2 for the two investigated current controllers. In the case of the hysteresis controllers the experimental results are equivalent with the corresponding virtual system results. However, in the case of the PI current regulators, some differences can be observed between the virtual and the experimental results. It can be seen that the current switching noise seems to be higher than in the previous cases. This is also proved by the current total harmonic distortion factor, having the higher value. However, there is not only switching noise present, but also current oscillations due to the faulty behavior of the PI current regulators. Also, the PHD value for the first 51 harmonics shows that the compensated current is also distorted, meaning the current is badly compensated, because the PI regulator bad operation affects the filtering efficiency. An interesting fact is the presence of harmonics left and right the 70th harmonic, which is half the PWM frequency. This harmonics are produced not by the switching operation of the active filter but by the current oscillations.

Table 2. Numerical results

Current regulator	THD_{uS} [%]	THD_{iS} [%]	$PHD_{iS\ 51}$	THD_{iL} [%]	FE
Hysteresis	2.09	6.32	2.71	15.77	2.49
PWM		11.50	9.53		1.42

5. Conclusion

Analyzing the virtual and experimental results, it can be concluded that the system performance is directly influenced by the control loops. It confirms that the hysteresis regulators can give good results, for a simple design and no tuning required, but with the cost of variable switching frequency. Another drawback is the need of a low time step for a numerically implemented regulator. At the same time, the PI regulators can give even better performance, but the poor experimental results proves the intricacy of the proportional-integrative control.

References

[1] Tenti P., Conservative Power Theory Seminar: A theoretical background to understand energy issues of electrical networks under non-sinusoidal conditions and to approach measurement, accountability and control problems in smart grids, UNICAMP – UNESP Sorocaba, August 2012.

[2] Popescu Mh., Bitoleanu A., Dobriceanu M., Lincă M., On the Cascade Control System Tuning for Shunt Active Filters Based on Modulus Optimum Criterion, Proc. of European Conference on Circuit Theory and Design, August 2009, Antalya, Turkey, pp. 137-140.

[3] Popescu Mh., Bitoleanu A., Dobriceanu M., Suru V., Optimum Control Strategy of Three-Phase Shunt Active Filter System, Proceedings of World Academy of Science, Engineering and Technology, Vol.58, Oct. 2009, pp. 245-250.

[4] Suru V., Popescu Mh., Pătraşcu C.A., Using dSPACE in the Shunt Static Compensators Control, Annals of The University of Craiova, No 37, 2013, pp 94-99.

[5] Ingram D., Round S., A Fully Digital Hysteresis Current Controller for an Active Power Filter, International Journal of Electronics, Vol 86, 1999.

[6] Suru C.V., Patrascu C.A., Popescu M., Bitoleanu A., Conservative Power Theory application in shunt active power filtering under asymmetric voltage, 14th International Conference on Optimization of Electrical and Electronic Equipment, 22-24 May 2014, Brasov, Romania

[7] Control Desk Experiment Guide for release 5.2, dSpace Gmbh, 2006.

Addresses:

- Lect. PhD. Eng. Constantin Vlad Suru, University of Craiova, Blvd. Decebal no. 107, RO-200440, Craiova, Romania, vsuru@em.ucv.ro
- Lect. PhD. Eng. Mihaita Linca, University of Craiova, Blvd. Decebal no. 107, RO-200440, Craiova, Romania, mlinca@em.ucv.ro
- Assist. PhD. Eng. Cristina Alexandra Patrascu, University of Craiova, Blvd. Decebal no. 107, RO-200440, Craiova, Romania, apatrascu@em.ucv.ro